ENGINEERING TRIPOS PART IIB PROF DAVID CARDWELL

Thursday 5th May 2011 2.30 to 4

Module 4C3 : ELECTRICAL AND NANO MATERIALS SOLUTIONS

1(a) The following explanation is very full. Full marks could be obtained for bullet point descriptions of these effects. Pyroelectric and piezoelectric materials are sub-classes of dielectrics, and are characterised by an asymmetry in their crystallographic structure, which leads to polar properties. The crystal structure of piezoelectric materials is characterised by a lack of centre of symmetry (i.e. they exhibit point or axial asymmetry). As a result, 20 of the known 21 dielectric structures that exhibit such a lack of centre of symmetry are piezoelectric.

Pyroelectricity, on the other hand, occurs in polar dielectric materials whose structure contains at least one *axis* along which an electric dipole moment exists. Only 10 of the 21 dielectric structures, therefore, exhibit pyroelectric properties (orthorhombic, tetragonal and triclinic, for example). A pyroelectric material is necessarily piezoelectric, although the converse is not true.

Both piezo and pyroelectric materials exhibit an intrinsic spontaneous polarisation, $\mathbf{P_S}$, which is given by the net electric dipole moment per unit volume, i.e.:

Microscopically, P_S originates from a structural transition which results in a displacement of the positive and negative centres of charge symmetry, i.e.:

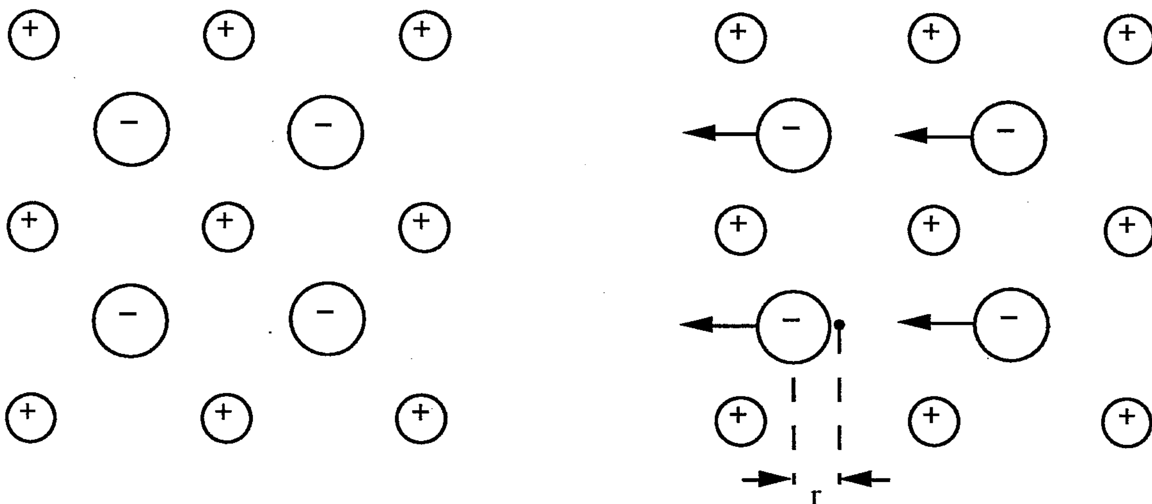

Non-polar lattice **Polar lattice**

Pyroelectricity is the change in polarisation that occurs in pyroelectric materials as their temperature changes. Quantitatively this is described in terms of the pyroelectric coefficient, **p**, which is given by the rate of change of $\mathbf{P_S}$, with temperature, i.e. the gradient of the $\mathbf{P_S}$ (T) curve;

$$\mathbf{p} = \frac{\Delta \mathbf{P_s}}{\Delta T} = \frac{d\,\mathbf{P_s}}{d\,T}$$

The piezoelectric effect can be described microscopically in a similar way to pyroelectricity, but driven by different extrinsic variables.

The majority of useful piezoelectrics and pyroelectrics are ferroelectric, since these have a number of polar axes and are therefore relatively easy to pole.

The direct piezoelectric effect is the production of a change in dielectric polarisation by the application of a mechanical stress. Conversely, application of an electric field to a piezoelectric will cause it to strain mechanically (indirect effect). [40%]

(b) Current responsivity is defined as; $R_i = \frac{i_p}{W_0}$ where i_p is the current which flows in an external circuit due to charge release associated with the temperature change. The detector operates under current mode at low frequencies (current has time to flow).

Voltage responsivity is defined as; $R_v = \frac{R_i}{Y} = \frac{i_p}{YW_0}$ where Y is the electrical admittance presented to i_p. The detector operates under voltage mode at high frequencies (current does not have time to flow).

$$\Delta T = \frac{\eta W_0 e^{i\omega t}}{G_T + i\omega H} \qquad i_p = A p \frac{dT}{dt} = \frac{\eta p A i \omega W_0 e^{i\omega t}}{G_T + i \omega H}$$

$$R_i = \frac{i_p}{W_0} = \frac{\eta p A i \omega e^{i\omega t}}{G_T (1 + i \omega \tau_T)} = \frac{\eta p A i \omega e^{i\omega t} (1 - i \omega \tau_T)}{G_T (1 + \omega^2 \tau_T^2)} \qquad \text{(Since } H = \tau_T G_T\text{)}$$

$$|R_i| = \left| \frac{\eta p A \omega e^{i\omega t} (i + \omega \tau_T)}{G_T (1 + \omega^2 \tau_T^2)} \right| = \frac{\eta p A \omega \sqrt{1 + \omega^2 \tau_T^2}}{G_T (1 + \omega^2 \tau_T^2)} = \frac{\eta p A \omega}{G_T \sqrt{1 + \omega^2 \tau_T^2}}$$

[30%]

(c) Sketch of variation of R_i with ω;

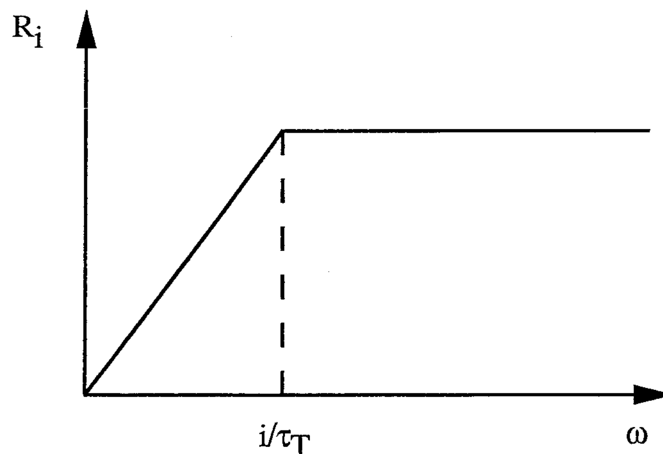

R_i is directly proportional to frequency for $\omega << 1/\tau_T$, i.e.;

$$\omega^2 \tau_T^2 << 1, \text{ so } \sqrt{1+\omega^2 \tau_T^2} \sim 1 \qquad \rightarrow \qquad |R_i| = \frac{\eta\, p\, A\, \omega}{G_T}$$

R_i is constant for frequencies >> $1/\tau_T$, i.e.;

$$\omega^2 \tau_T^2 >> 1, \text{ so } \sqrt{1+\omega^2 \tau_T^2} \sim \sqrt{\omega^2 \tau_T^2} = \omega\, \tau_T \quad \rightarrow \qquad |R_i| = \frac{\eta\, p\, A}{G_T\, \tau_T} = \frac{\eta\, p}{c\, d}$$

($\tau_T = H/G_T$ and $H = c\ d\ A$) [10%]

(d) In the frequency-independent regime ($|R_i|$ = constant); $|R_i| = \dfrac{\eta\, p\, A}{G_T\, \tau_T} = \dfrac{\eta\, p}{c\, d}$

For $t = 30\ \mu\text{m}$ and $\eta = 0.95$, $p = 230\ \mu\text{Cm}^{-2}\text{K}^{-1}$ and $c = 3.2\ \text{MJm}^{-3}\text{K}^{-1}$;

$$|R_i| = \frac{0.95 \times 230 \times 10^{-6}}{3.2 \times 10^{6} \times 30 \times 10^{-6}} \sim \mathbf{2.28 \times 10^{-6}\ A\ W^{-1}}$$ [20%]

A popular and straightforward question, answered very well by most candidates. Common sources of lost marks were for lack of detail in describing the microscopic properties in part (a) and for numerical errors in part (d).

2.(a) The following explanation is very full. Full marks could be obtained for bullet point descriptions of these effects. Hard permanent magnet materials, such as Nd-Fe-B or $SmCo_5$, contain pinning centres that inhibit the movement of domain walls, and hence have a high coercive field, H_c (of the order of 100 kAm^{-1}). Hard permanent magnets are able to retain their magnetisation and are able to resist the effects of de-magnetisation. As a result, they are used primarily in short, fat geometries. Soft permanent magnet materials, such as pure iron and permalloy, contain very few domain wall pinning centres and, as a result, are unable to resist the effects of de-magnetisation. They have a low H_c (of the order of Am^{-1}) and are used typically in long, thin geometries. The remanent field associated with hard permanent magnetic materials is typically lower than that associated with soft materials (< 1T, compared to > 1T). [15%]

(b) Variation of flux density with applied field for hard and soft permanent magnet materials over a full field cycle;

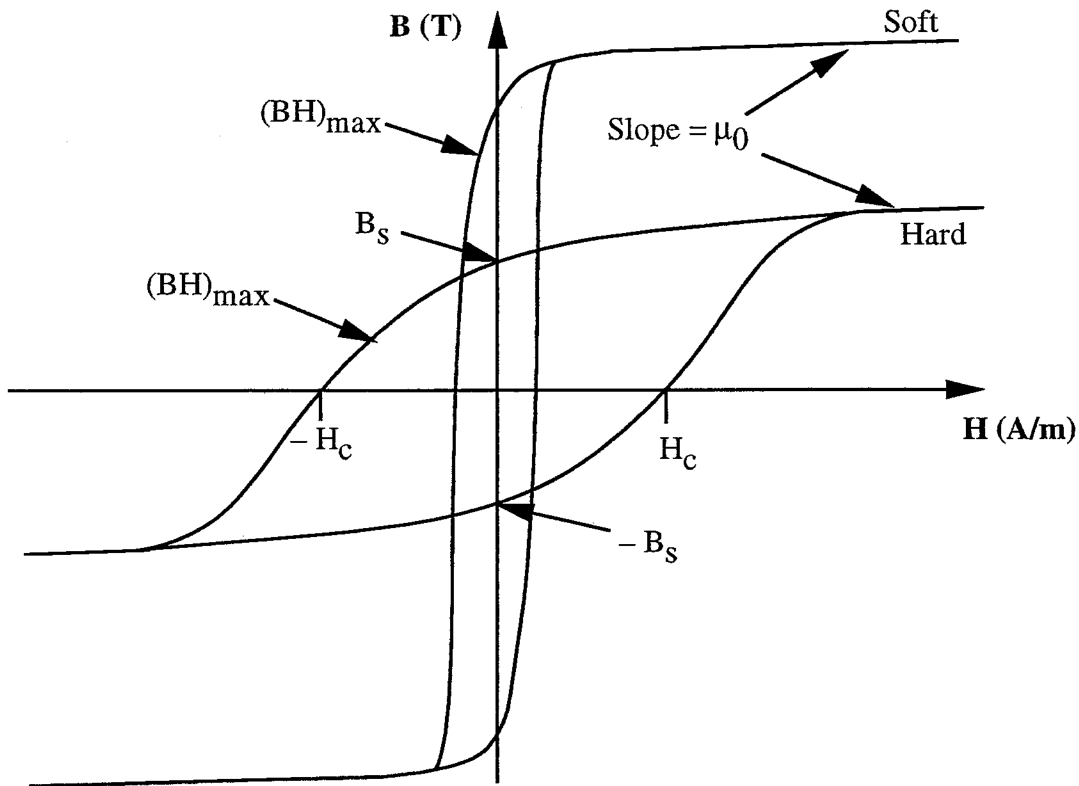

Key features; B_s - saturation flux density

H_c - strength of domain wall pinning centres (i.e. microstructural imperfections)

Loop area = energy density per cycle

$(BH)_{max}$ occurs closer to the B axis for soft materials and closer to the H axis for hard materials.

[20%]

(c) Magnet geometry determines the demagnetising factor of a permanent magnet (N = 0 for a long, thin cylinder magnetised along its length and N = 1 for a thin plate magnetised across its thickness). This, in turn, determines the value of H in the second quadrant of the

B-H curve, and hence the associated value of B. Permanent magnets are applied optimally at the maximum value of the product of B and H (i.e. BH_{max}), which occurs at different values of H for hard and soft permanent magnet materials [see sketch in part (c)]. BH_{max} occurs at high H for hard permanent magnet materials, corresponding to the operating point for geometries with high demag factors. Conversely, BH_{max} occurs at low H for soft permanent magnet materials, corresponding to the operating point for geometries with low demag factors.

Applications of hard permanent magnet materials include (i) rotors for dc permanent magnet motors, (ii) magnetic sensors in alarm systems, (iii) fridge magnets, (iv) generators in Faraday devices such as 'kinetic' watches and torches, (v) water pumps in washing machines and (vi) magnetic stirrers and holders (2 examples required).

Applications of soft permanent magnet materials include (i) transformer cores, (ii) magnetic shielding in MRI, (iii) magnetic circuits in motors and generators, (iv) electromagnets and(v) linear motors (2 examples required). [20%]

(d) Magnetic flux density is generated in bulk superconductors by the Faraday effect. This involves applying a changing magnetic field to the superconductor, which induces an e.m.f., which causes an Eddy current to flow throughout the bulk material. The Eddy current, in turn, generates magnetic flux. As a result, bulk superconductors generate fields in a way analogous to wire-wound solenoids.

A bulk type II superconductor can be magnetised *either* by cooling in an applied magnetic field of magnitude at least the equal to the maximum trapped field and then removing the field (the field cooling, or FC, method) *or* by cooling the superconductor in the absence of a magnetic field (zero field cooled, or ZFC) and then applying and removing a field of magnitude at least twice that of the maximum trapped field. [20%]

(e) (i) The field generated at the centre of the long solenoid is given by;

$$B = \mu_0 \frac{N}{L} I = 4\pi \times 10^{-7} \times \frac{5000}{0.15} \times 5 = 0.21 \text{ T}$$

(ii) The field generated at the surface of the YBCO disc is given by;

$$B = \mu_0 \frac{J_c d}{4} = 4\pi \times 10^{-7} \times \frac{30 \times 10^7 \times 0.02}{4} = 1.88 \text{ T}$$

The superconductor generates approximately 9 × the field of the solenoid.

The factors that may limit realising these fields are;

Solenoid: Coil heating effects, which will reduce the current or cause the coil to melt. YBCO: Bursting stress (pr/t) due to the magnetic pressure (YBCO is brittle, with a relatively low fracture toughness) and field dependence of J_c, which will reduce the trapped field at the surface of the cylinder. [25%]

A popular question. Candidates referred infrequently to the movement of domain walls in part (a). Part (b) was answered well, although the position of BH_{max} was often overlooked in part (c). Most answers focused on the zero field cooling magnetisig technique in part (d). The calculation in part (e) was generally done well.

3(a) See lecture notes. ALD is a CVD-based technique that allows atomic level thickness control by breaking the CVD process into two, self-limiting (half) reactions. For CVD using binary reactions, the A and B reactants are present at the same time and form the product film continuously on the substrate. In ALD, the substrate is exposed to the A and B reactants individually and the product film is formed in a stepwise and digital fashion. [15%]

(b) (i) For a surface-reaction controlled regime the deposition rate $R \approx \exp(-E_a/kT)$, hence $R(800°C) = R(700°C)\times[\exp(-2eV/(k\times1073K))/ \exp(-2eV/(k\times973K))] \approx 920$ nm/s. [10%]

(ii) At high temperatures (here 800°C) the CVD process becomes mass transfer controlled. The mass transfer coefficient is thereby proportional to gas diffusivity which has an approx. $T^{3/2}$ dependence, i.e. the gradient of the graph of deposition rate as a function of 1/T is much lower.

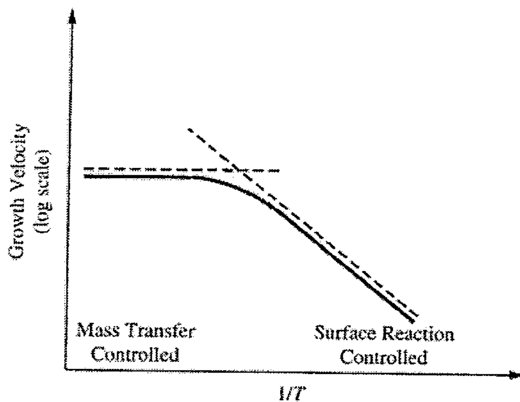

[25%]

(c) The dominant elastic interaction of primary electrons is Rutherford scattering for which the differential cross section is approximately proportional to Z_{target}^2, i.e. a higher atomic number leads to a greater Coulombic attraction. Hence the 20 keV electrons undergo a greater degree of scattering per unit length in Au, reducing the interaction volume. In addition the scattering angles in Au are larger. Figure 1(a) (left) shows trajectories for C, Fig. 1(b) (right) for Au. [20%]

(d) See lecture notes. A high-energy primary electron creates a vacancy in the inner shell of electrons of the scattering atom. An electron from an outer shell fills this vacancy and thereby an X-ray is emitted with an energy characteristic of that electron transition of the element. The EDS detector measures the energy and intensity of the X-rays emitted during this process, thus identifying the element and its concentration. The rough magnitude of core energy levels can be estimated from $E=13.6\ Z^2/n^2$ [eV], where Z is atomic number and n is principle quantum number. For an element with Z = 50 the energy required to expel an electron from an inner shell is $13.6\times50^2 = 34$ keV. However, electrons are ≈1/1800th of the mass of a single proton so very little momentum is transferred and relatively little damage is done to the sample. [20%]

(e) Other techniques include Auger electron spectroscopy (AES), X-ray photoelectron spectroscopy (XPS), secondary ion mass spectroscopy (SIMS), Rutherford back scattering (RBS). See lecture notes for details. [10%]

Only two candidates attempted this question. Parts (a), (d) and (e) were generally well answered, although candidates lost some points by not giving all details. Part (b)(i) was poorly answered, which is surprising as it just requires filling in values into two exponentials. Also Part (c) was poorly answered. Candidates thought about the electrical conductivity of Au rather than the cross section for scattering. Part (b)(ii) was answered very well by the IIB candidate, not the candidate for the graduate progress examination.

4(a) Si

Advantages: cheap, SiO_2 as oxide, versatility, moderate speed, bipolar.
Disadvantages: slow, indirect gap, not opto-electronic.

GaAs

Advantages: faster than GaAs, lower effective mass.
Disadvantages: cost, small wafer sizes, bad oxide, not passivated, complicated defects.

GaN

Advantages: faster than Si, high thermal conductivity, high breakdown field, bipolar, high figure of merit for power devices, wide band gap, direct gap, opto-electronic, LEDs.
Disadvantages: poor oxide, deep acceptors, processing, cost, small wafer sizes. [30%]

(b)

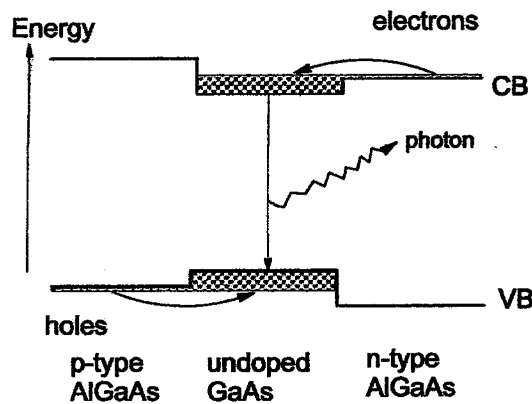

[15%]

(c)

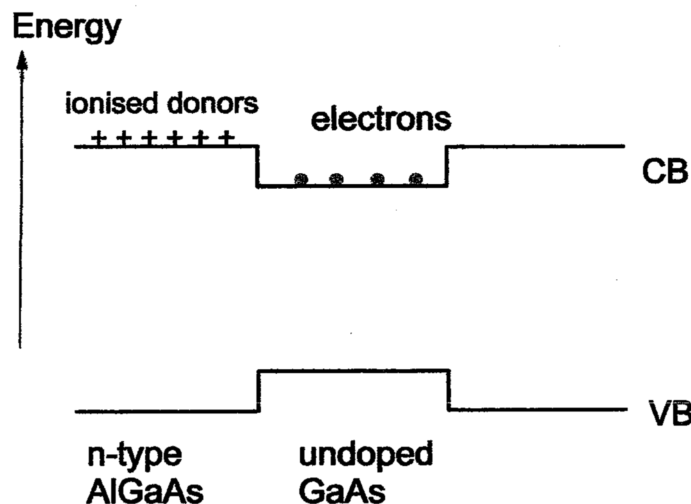

Donor electrons are transferred from a wide gap material with the donors, into narrower gap intrinsic material. This separates electrons from the positive donor ions, reduces Coulombic scattering, and thereby increases mobility. (ADD LIMIT TO CHOICE OF MATERIAL) [15%]

(d) Matching is needed to avoid dislocations;

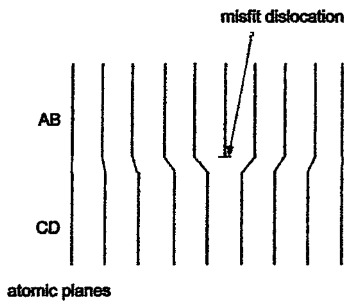

Band gaps vary roughly inversely with lattice constant.

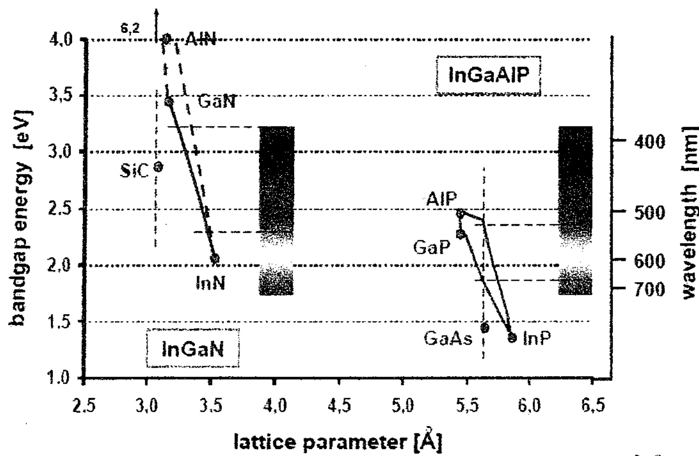

Fraction of dislocations = $\delta d/d$. Thus spacing of dislocations = $d/\delta d$ unit cells, or $d^2/\delta d$ Angstroms. [40%]

This was a question about the relative merits of Si, GaAs and GaN as semiconductors, and about heterostructures for LEDs and HEMTs and the problems of lattice matching. The question was reasonably popular and the candidates generally understood the question and gave reasonable answers.

5(a) Substitutional doping: The number of electrons donated to the bands = Z-4 for Si, where Z is the valence of the dopant, 4 is the valence of Si. For interstitial doping, the number of electrons donated = Z, as the host interstitial is like a blank atom.

For Si, the donors are group V elements (P, As etc), and group III elements (B, Al etc) are the acceptors. For interstitials, alkali metals (Li) are donors, acceptors don't work.

For III-Vs, the number of electrons donated = Z- 5 for dopants on the V site, and =Z-3 for dopants on the III site. Hence Si acts as a single donor on the Ga site, and Se on As acts as a donor, while Mg on a Ga site would act as an acceptor.

[15%]

(b) For an ionised dopant in Si, the core charge is +(Z-4). This ion acts like a proton in the H atom. But whereas the proton and electron is in a vacuum or 'free space' where the Coulomb force is screened by free space, in the solid the Coulomb attraction is screened by the actual optical dielectric constant (ambient) of Si. Also, the electron wavefunction is expressed in terms of wavefunctions drawn from the band extrema, so that we replace the free space electron mass by the effective mass m* in the solid.

Hence the normal Rydberg energy (binding energy) of the electron of the hydrogen atom

$$R_0 = \frac{e^4 m}{32\pi^2 \varepsilon^2 \hbar^2} = 13.6 \text{ eV}$$

Becomes rescaled by the Si values of ε and m*

$$R = R_0 m^*/\varepsilon^2.$$

Values for electrons in Si are very different from 1, ε=12 and m* = 0.08, so that $R = 45$ meV. This is very small and so R is comparable to the thermal energy, $kT = 25$ meV which explains that donors and acceptors are easily ionised at room temperature in Si and typical semiconductors. Doping of Si and Ge is easy. This is not true of all other semiconductors.

[30%]

(c) The 3 mechanisms that limit doping are;
solubility
deep levels
compensation by other defects.

Si only deep/solubility (m* is low).
GaAs deep/solubility (m* is low).
ZnO compensation/deep for acceptors (m*e is low, m*h is high).
HfO_2 no doping – everything is deep and compensated (both m* are high). [30%]

(d)

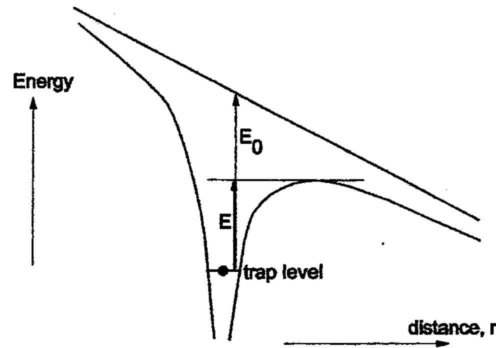

Poole-Frenkel. This diagram shows the effect of a high electric field on an electron bound in a deep state in the band gap of an insulator. To give conductivity, the electron must escape the being bound. It does this by excitation over the energy barrier indicated. The size of this barrier depends on the electric field, and it is

$$E = 2\left(\frac{e^2}{4\pi\varepsilon}\right)^{1/2} F^{1/2}$$

This leads to conduction proportional to

$$J \sim j_0 \exp(-(E_0 - 2(e^2/4\pi\varepsilon)^{1/2} F^{1/2})/kT)$$

On the other hand, for larger band gaps, the conduction is limited by the interface between the metal /semiconductor and the insulator. This leads to conduction that is inversely proportional to the barrier height at the interface, ϕ eV.,

$$J = j_0 \exp(- a\phi^{3/2}/F)$$

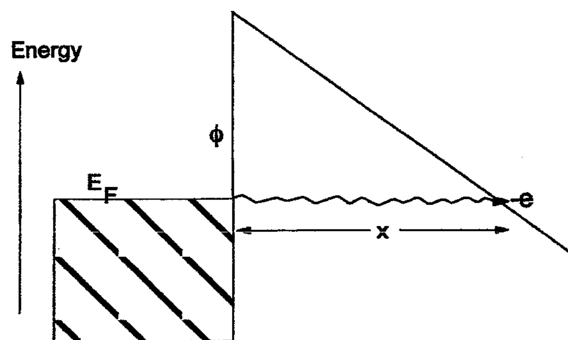

Analysis –

$x = \phi / F$

$$\frac{\hbar^2 k^2}{2m} = -\phi$$

or $k = (2m\phi)^{1/2}/\hbar$

Now

$j = j_0 \exp(-2|k|x) = j_0 \exp(-2(2m\phi)^{1/2}.\phi/(F\hbar))$

$= j_0.\exp(-2^{3/2}m^{1/2}\hbar^{-1}\phi^{3/2}/F)$

The final mechanism is Schottky emission. This occurs for smaller barriers than *Fowler-Nordheim tunnelling*. It occurs by thermal emission over the barrier, not tunnelling, and gives an equation very similar to that of Poole-Frenkel conduction.

[25%]

This was a question about doping, the effective mass model of dopant levels, and whether dopants give shallow or deep levels in different materials. This was also a reasonably popular question, which was typically answered well. However, the last part of the question on conduction in insulators was not answered well and was missed in a number of cases.